

IN SITU AND POST REACTION COBALT-INCORPORATION INTO AMINOPROPYL-MODIFIED PERIODIC MESOPOROUS ORGANOSILICA MATERIALS

Alufelwi M. Tshavhungwe and Neil J. Coville*

DST/NRF Centre of Excellence in Strong Materials and the Molecular Sciences Institute,
School of Chemistry, University of the Witwatersrand, Johannesburg, 2050, South Africa

(Received March 1, 2005; revised May 4, 2005)

ABSTRACT. Bifunctional periodic mesoporous organosilica materials with and without cobalt ion incorporation were synthesized by co-condensation of 1,2-bis(trimethoxysilyl)ethane (BTME) with 3-aminopropyltriethoxysilane (APTS) in the presence of cetyltrimethylammonium bromide. Cobalt was incorporated onto APTS-modified ethylene-bridged silica materials by *in situ* and by incipient wetness addition methods. The periodicity of the new materials is indicated by the presence of low angle diffraction peaks found in the XRD profiles (pore size ca. 40 nm). The surface area, pore volume and pore diameter of the new ethylene-bridged silica materials decreased with increasing loading of APTS as well as after cobalt incorporation. Thermogravimetric analysis and Raman spectroscopy show that the surfactant is removed by solvent extraction. Cobalt ion incorporation is confirmed by Raman spectroscopy and UV-vis diffuse reflectance spectroscopy.

KEY WORDS: Bifunctional periodic mesoporous organosilica, 1,2-bis(trimethoxysilyl)ethane, 3-aminopropyltriethoxysilane, Sol-gel, Cobalt

INTRODUCTION

The sol-gel method is widely used to synthesise periodic mesoporous organosilica (PMOs) materials containing both bridging organic functional moieties in the framework and terminal organic functional groups protruding into the channel pores [1 – 20]. The large ordered pore sizes of PMOs make these materials very attractive for applications such as catalyst supports, sensors and adsorbents for heavy metal ions. Periodic ethylene-bridged silica materials, by far the most widely studied PMO, has been modified by co-condensation of 1,2-bis(trimethoxysilyl)ethane precursors with various trialkoxyorganosilanes in the presence of surfactants [21 – 32]. Organosilane precursors co-condensed with bis(trimethoxysilyl)ethane include 3-glycidopropyltrimethoxysilane [21], 3-cyanopropyltriethoxysilane [22], N-(2-aminoethyl)-3-aminopropyltrimethoxysilane [H₂N-(CH₂)-NH(CH₂)₃] [26], N-[3-(trimethoxysilyl)propyl]ethylenediamine [27] and mercaptopropyltrimethoxysilane [HS-(CH₂)₃-] [26, 31, 32].

PMO materials containing “nitrogen-bearing” functional groups (e.g. cyano- (CN) [22], amines (NH) [24 – 27, 33], etc) have also received some attention. Asefa *et al.* prepared periodic mesoporous aminosilicas that contain amine functional groups in the framework of a mesoporous network via thermal ammonolysis of periodic mesoporous organosilicas (PMOs) under a flow of ammonia gas [33]. Burleigh and co-workers described the preparation of a porous organosilica by co-condensation of bis(trimethoxysilyl)ethane and N-(2-aminoethyl)-3-aminopropyltrimethoxysilane, N-[3-(trimethoxysilyl)propyl] ethylenediamine or Cu(II)-complexed N,N'-bis[3-(trimethoxysilyl)propyl]ethylenediamine under acidic and basic conditions [24 – 27].

*Corresponding author. E-mail: neilcoville@yahoo.com or ncoville@aurum.chem.wits.ac.za
Fax: +27 11 717 6749. Tel.: +27 11 717 6738.

For catalytic applications, aminopropyl-functionalised amorphous and ordered mesoporous silicas have been the most widely studied organic-inorganic hybrid solids [34]. These organic-inorganic hybrids have been used as catalysts for the Knoevenagel condensation of various aldehydes and ketones with ethyl cyanoacetate [35 – 37] as well as for base-catalysed reactions such as the nitroaldol condensation and Michael addition reactions [38, 39].

Although unfunctionalized silica materials, including ordered mesoporous silicas (MCM 41) have been used as supports for cobalt-based catalysts in the Fischer Tropsch (FT) synthesis [40 – 42], there are very few reports in the literature on cobalt incorporation into periodic mesoporous organosilica materials. Further, amine functionalised silicas have not been used in the FT reaction.

Herein we report on the synthesis and characterization of organosilica materials synthesized by co-condensation of 1,2-bis(trimethoxysilyl)ethane (BTME) with 3-aminopropyltriethoxysilane (APTS) in the presence of hexadecyltrimethylammonium bromide (cetyltrimethylammonium bromide, CTAB) as the surfactant both in the presence and absence of cobalt ions. The molecular structures of these silica precursors and the surfactant are shown in Scheme 1. Cobalt ion was added to the formed silicas to generate Co supported catalysts for use in Fischer-Tropsch (FT) synthesis [43 – 47]. 3-Aminopropyltriethoxysilane (APTS) has a terminal amine group which may be beneficial for binding metals and this is one of the aspects of APTS which we wish to explore in this study.

The FT studies are a continuation of previous studies on Co supported catalysts [48, 49]. To the best of our knowledge, this is the first report on the synthesis of cobalt ion incorporated APTS-modified ethylene-bridged silica.

EXPERIMENTAL

Chemicals

1,2-bis(trimethoxysilyl)ethane (BTME), hexadecyltrimethylammonium bromide (CTAB) and cobalt nitrate hexahydrate were obtained from Aldrich; 3-aminopropyltriethoxysilane (APTS) was obtained from ABCR (Germany). All chemicals were used as received.

Synthesis

APTS-functionalized ethylene-bridged silica materials. PMOs were prepared using a modified method based on that reported by Ozin and co-workers [23]. A series of APTS-modified ethylene-bridged silica materials were prepared starting with a mole ratio of BTME:APTS:CTAB:NH₄OH:H₂O = 1: x: 0.275: 64: 218 (where x = 0, 0.476, 0.714, and 0.952). In a typical synthesis, CTAB (0.36 g; 0.98 mmol) was dissolved in a solution consisting of water (14 mL) and 28 % ammonium hydroxide (8 mL; 0.229 mol). The mixture was stirred for 45 minutes. The pH of the solution was estimated by pH paper to be approximately 10. A mixture of BTME (0.9 mL, 3.57 mmol) and APTS [varying amounts: 0.8 mL (3.40 mmol), 0.6 mL (2.55 mmol) and 0.4 mL (1.70 mmol)] was added dropwise to the stirred mixture. These materials are denoted as BAA(1:1), BAA(1:0.7) and BAA(1:0.5), respectively (see section *Nomenclature* for a description of notation used). Stirring was continued for a further 1 hour, followed by ageing at 80 °C for 4 days. The solid was suction filtered in a Buchner funnel and washed with an excess of water. The solid was dried in air overnight to give the required material (between 1 and 2 g).

Surfactant extraction. A portion of the as synthesized sample (0.5 g) was stirred in a solution of concentrated HCl (5 mL) in methanol (200 mL) at 50 °C for 2 days. The solid was suction filtered in a Buchner funnel, washed with water and finally with methanol (200 mL) and then dried in air. Mass losses of between 20 and 40 % were observed after surfactant extraction. Extracted materials are denoted as BAE(1:1), BAE(1:0.7) and BAE(1:0.5), respectively.

***In situ* cobalt incorporated APTS-functionalized ethylene-bridged silica.** Cobalt incorporated APTS-modified ethylene-bridged silica materials were synthesized by adding cobalt nitrate [0.1 g; 0.34 mmol] to a reaction mixture of CTAB (0.36 g; 0.98 mmol), water (28 mL) and 28 % ammonium hydroxide (8 mL; 0.229 mol). A mixture of BTME and APTS (BTME:APTS = 1:1 or 1:0.5) was then added dropwise to the mixture. The procedure, including solvent extraction, was continued as described above for the synthesis of APTS-modified ethylene-bridged silica materials. The APTS-modified ethylene-bridged silica materials synthesized in this manner are denoted as 6.7CoBAE(1:1)-*in situ* and 6.7CoBAE(1:0.5)-*in situ*. The corresponding ethylene-bridged silica (not modified) is denoted as 6.7CoBE-*in situ*.

Post reaction cobalt incorporated APTS-functionalized ethylene-bridged silica. Cobalt incorporated aminopropyl-modified ethylene-bridged silica was prepared using the incipient wetness impregnation method. An aminopropyl-modified ethylene-bridged silica [BAE(1:1)] having a BET surface area, pore volume and desorption BJH pore diameter of 389 m²/g, 0.27 cm³/g and 3.0 nm, respectively, was used as the support. Different amounts of cobalt nitrate, Co(NO₃)₂·6H₂O, (0.1 g and 0.2 g) were dissolved in deionised water and impregnated into the support (0.3 g) using incipient wetness to give materials with 6.7 % and 13.5 % cobalt. Materials were dried at 120 °C for 12 hours. Materials synthesized in this manner are denoted as 6.7CoBAE(1:1)-*imp* and 13.5CoBAE(1:1)-*imp*.

Nomenclature. The percentage APTS indicates the percentage of APTS expressed per mole of silicon atoms in the BTME and APTS organosilica precursors { % APTS = [100 x (mol Si in APTS)/(2 x moles Si in BTME + mol Si in APTS)]}. The moles of BTME are multiplied by 2 because each BTME molecule supplies two moles of Si whereas an APTS molecule supplies one. The notation used to identify the samples is as follows: A = APTS, B = BTME, Co = cobalt, A = as synthesized, and E = extracted. The mole ratio of BTME to APTS in the reaction mixture is given in parenthesis. Numerical figures preceding Co refer to the percentage of cobalt in the sample in cobalt incorporated samples. The method used to incorporate cobalt is identified by *imp* (impregnated) or *in situ* after the name. For example, BAE(1:0.5) refers to an extracted (*E*) sample synthesized from APTS (*A*) and BTME (*B*) in which the ratio of BTME to APTS is 1:0.5. 6.7CoBAE (1:1) – *imp*, refers to a cobalt incorporated (6.7 % *Co*), extracted (*E*) material synthesized from APTS (*A*) and BTME (*B*) in a 1:1 ratio in which cobalt was supported by impregnation (*imp*).

Characterization

Powder X-ray diffraction. Powder X-ray diffraction measurements were made on a Phillips PW1710 diffractometer with Cu K- α radiation ($\lambda = 1.5443 \text{ \AA}$). Powdered disc samples were analysed at a scan speed of 5° s⁻¹ in the 1.5 – 10° or 1.5 – 70° 2 θ range at a generator voltage of 40 kV and a generator current of 20 mA.

Nitrogen sorption. The nitrogen adsorption and desorption isotherms were measured at –196 °C using a Micromeritics ASAP2010 instrument. Prior to adsorption measurements, all samples were degassed for 12 hours at 120 °C. The BET surface area was calculated from the adsorption

isotherm in a relative pressure range from 0.001 to 0.20. The total pore volume was evaluated from the amount of nitrogen adsorbed at a relative pressure of 0.98. The average pore diameter was evaluated by the BET method (4V/A). The pore size distribution was obtained from analysis of the adsorption and desorption branches of the isotherm using the Barrett-Joyner-Halenda (BJH) method.

Thermogravimetric analysis. Thermogravimetric analyses were performed with a Perkin Elmer Pyris 1 TGA Thermogravimetric analyser using nitrogen or air as the purge gas at a heating rate of 5 °C per minute.

Raman spectroscopy. Measurements were made using the micro-Raman attachment of a Jobin-Yvon T64000 Raman spectrometer, configured in single spectrograph mode. A grating with 600 grooves/mm was used to disperse the spectrum onto a charge coupled device (CCD) detector. The laser spot size on the sample was ~1.5 microns in diameter, and the excitation wavelength was 514.5 nm from an argon ion laser.

Scanning electron microscopy. SEM images were recorded on a JSM 840 Scanning Electron Microscope with an acceleration voltage of 10 kV and a working distance of 15 mm. Prior to measurements, the samples were sprinkled on a disk smeared with carbon and then coated with gold.

UV-vis diffuse reflectance spectroscopy. UV-Vis diffuse reflectance spectra were recorded with a Cary-5E Varian spectrometer equipped with a Praying-Mantis diffuse reflectance attachment. BaSO₄ was used as reference.

RESULTS AND DISCUSSION

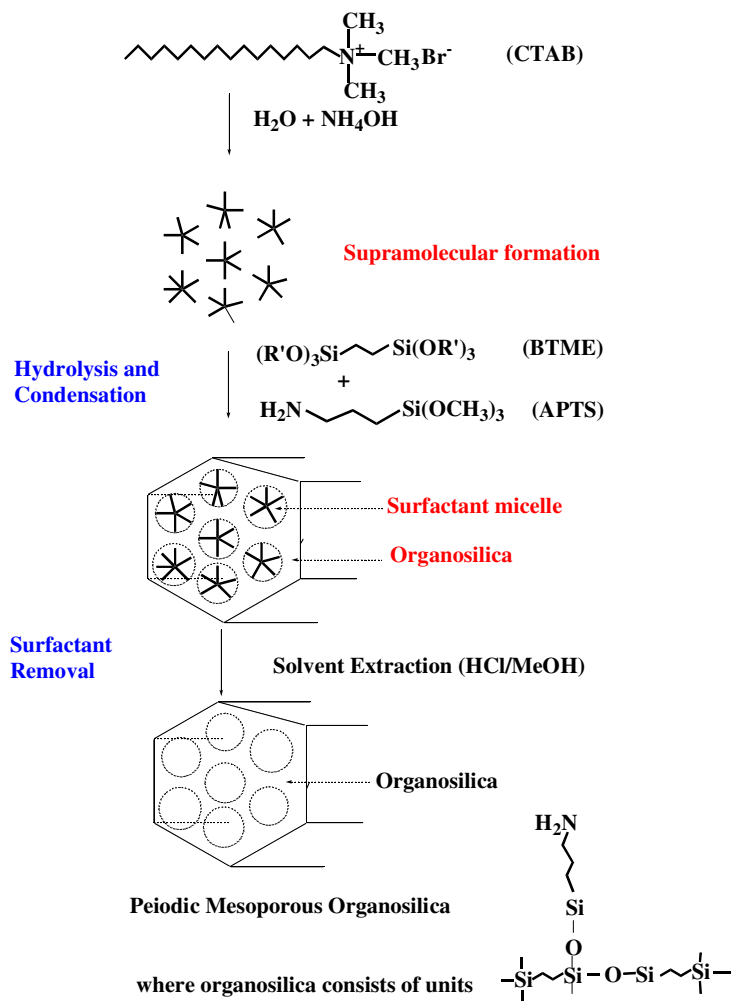
Synthesis

Addition of a mixture of BTME and APTS to a basic solution of CTAB formed white solid materials. A gel formed immediately for samples containing large amount of APTS. For all mixtures, precipitation started within 30 minutes after addition of the silica precursor. Addition of cobalt nitrate to the mixture yielded dark brown/black materials for CoBAE(1:0.5)-*in situ* and CoBAE(1:1)-*in situ*. The base-catalysed surfactant-templated formation of APTS-modified periodic mesoporous ethylene-bridged silica is proposed to form from micelles [50] as illustrated in Scheme 1.

Powder X-ray diffraction

APTS-modified ethylene-bridged silica. Powder XRD was used to probe the periodicity of the mesoporous materials. Periodic mesoporous materials display a very high intensity peak at around $2\theta = 2^\circ$, together with low intensity peaks below 8° [50, 51]. The prominent low angle peak at approximately $2\theta = 2^\circ$ indicates the presence of uniformly sized pores for ordered materials. XRD patterns (shown in Figure 1) show relatively broad low angle peaks compared to that of hexagonal MCM 41 materials. The absence of higher angle reflections suggests the lack of long range order. The most intense peak was arbitrarily assigned as the d (100) peak. Powder XRD patterns of the as synthesized and the solvent extracted APTS-modified ethylene-bridged silica samples in which the BTME:APTS mole ratio is 1:1 are shown in Figure 1 (D and C, respectively; d values of 3.9 and 4.1 nm, respectively). Corresponding values obtained for a

related amine-functionalised material synthesized by Burleigh *et al.* [26] are 4.3 nm and 4.4 nm, respectively, and suggests equivalent structures.



Scheme 1. Reaction scheme showing the formation of periodic mesoporous aminopropyl-modified ethylene-bridged silica. Note that the framework is made up of units of $\text{H}_2\text{NCH}_2\text{CH}_2\text{CH}_2\text{SiO}_3$ and $\text{O}_3\text{SiCH}_2\text{CH}_2\text{SiO}_3$.

As expected for organic-functionalized silicas synthesized via co-condensation [23, 52], the position of the d (100) peak shifts to higher angles (implying lower d values) as the amount of APTS added increased (Table 1). This shift corresponds to the reduction in the interplanar spacing from about 4.9 to 3.9 nm for BAE(1:0.5) and BAE(1:1), respectively. The same behaviour was observed for BTME silica modified by co-condensation with various

organosilanes including 3-glycidoxypropyltrimethoxysilane [21] and 3-cyanopropyltriethoxysilane [22].

From the above data it can be seen that the amount of APTS has an effect on the pore structure of the silica material. It is assumed that the major effect arises from an interaction of the CTAB micelle with the APTS that modifies the micelle structure, leading to the loss of long range order. Increasing the amount of APTS may cause an increase in the number of electrostatic interactions between the aminofunctional group of APTS and the quaternary ammonium head group of the surfactant, which can result in a change in the density of silanol groups in the surfactant silicate interface, thereby requiring fewer surfactant molecules for charge balance. This situation leads to contraction of the micelle size in hybrid mesoporous materials with higher concentrations of APTS [22, 53]. However, further work on this and other related systems will need to be performed to confirm this suggestion.

It was also observed that when the ratio of surfactant to silica precursors was changed, by increasing the amount of surfactant while keeping the amount of silica precursors constant, the d_{100} peak observed in the surfactant-containing material (with a reduced intensity) disappeared after solvent extraction.

Co-incorporated APTS-modified ethylene-bridged silica. The XRD pattern of a solvent-extracted material synthesized in the presence of cobalt nitrate (0.1 g) using a BTME:APTS mole ratio of 1:0.5, CoBAE(1:0.5)-*in situ*, displays an intense diffraction peak with a lattice spacing, d_{100} , of 4.78 nm at 1.85° (Figure 1B). This value is slightly higher than that of BAE(1:0.5) (Figure 1A), by ~ 0.1 nm. As shown in Figure 1 (insert), the material obtained by impregnating 0.3 g of the material prepared from a BTME:APTS mole ratio of 1:1 with 0.1 g cobalt nitrate [6.7CoBAE(1:1)] does not show any low angle diffraction peaks, suggesting loss of mesophase for this sample. Similar results were reported for other Co-impregnated ethylene-bridged silica materials [54].

Table 1. Structural properties of organosilica materials.

Sample and % APTS ^a	SA ^b (m ² /g)	PV ^c (cm ³ /g)	APD ^d (nm)	D _{ad} ^e (nm)	D _{des} ^f (nm)	d_{100} ^g (nm)
BAE(1:1) [32 %]	389	0.27	2.78	2.1 – 2.2 (2.0)	3.0 – 2.9 (3.0)	3.92 (4.11)
BAE(1:0.7) [26 %]	426	0.30	2.83	1.7 – 1.7 (1.7)	2.6 – 2.1 (2.3) ^h	4.38
BAE(1:0.5) [19 %]	470	0.45	3.82	2.8 – 2.6 (2.7) ^h	3.2 – 3.1 (3.2)	4.93
BE	672	0.71	4.24	2.2 – 2.1 (2.2)	3.3 – 3.2 (3.3)	4.75 (4.42)
13.5CoBA(1:1) – <i>imp</i>	181	0.14	2.53	2.0 – 1.8 (1.9)	3.1 – 3.0 (3.1)	
6.7CoBAE(1:1)- <i>imp.</i>	250	0.17	2.76	1.9 – 1.8 (1.8)	3.2 – 3.1 (3.1)	
6.7CoBAE(1:1)- <i>in situ</i>	308	0.19	2.52	- ⁱ	-	4.34
6.7CoBE - <i>in situ</i>	438	0.48	4.34	2.5 – 2.4 (2.4)	3.2 – 3.1 (3.1)	4.45

^a Values in square brackets are % APTS = [100 x (mol Si in APTS)/(2 x moles Si in BTME + mol Si in APTS), ^b SA = BET Surface Area, ^c PV = Total Pore volume (cm³/g), ^d APD = Average Pore Diameter, ^e D_{ad} = BJH Adsorption Pore Diameter, ^f D_{des} = BJH Desorption Pore Diameter, ^g d_{100} = XRD lattice parameter of extracted samples. The value of the corresponding as synthesized sample is given in parenthesis. ^h Broad PSD 'mesopore' peak. ⁱ Not determined, 5-point BET method was used to determine surface area.

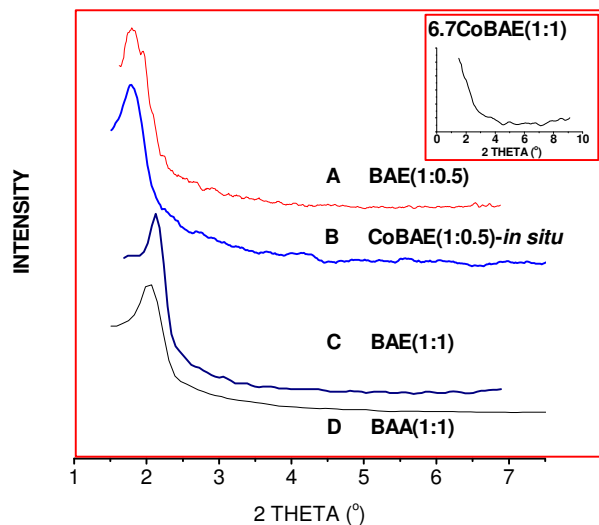


Figure 1. XRD patterns for aminopropyl-functionalized ethylene-bridged silicas. A = extracted APTS-modified ethylene-bridged silica (BTME:APTS = 1:0.5); B = extracted APTS-modified ethylene-bridged silica (BTME:APTS = 1:0.5) prepared in the presence of 0.1 g cobalt nitrate; C and D = extracted and as-synthesised APTS-modified ethylene-bridged silicas (BTME:APTS = 1:1), respectively. Insert: APTS-modified ethylene-bridged silica (BTME:APTS = 1:1) impregnated with 0.1 g cobalt nitrate.

Nitrogen sorption

APTS-modified ethylene-bridged silica. Nitrogen adsorption-desorption isotherms for extracted aminopropyl-modified ethylene-bridged silica samples with BTME:APTS mole ratios of 1:0.5, 1:0.7 and 1:1 in the synthesis gels are shown in Figure 2 (A, B and C, respectively). All the materials exhibit Type IV isotherms with a narrow pore size distribution according to the IUPAC classification, which is typical for mesoporous materials [55]. The shape of the hysteresis loop (Type H4) observed for BAE (1:1) and BAE (1:0.7) is consistent with the presence of ‘ink-bottle’ pores having a narrow entrance and wide interior.

The structural properties (BET surface area, average pore diameter, pore volume and lattice parameter) of these materials are listed in Table 1. BJH desorption PSDs with maxima ranging between 3.3 (for the unmodified ethylene-bridged silica material) and 3.0 nm (for the material with BTME:APTS = 1:1) are obtained. (Table 1, Figure 2). The corresponding pore diameters obtained from the adsorption isotherm are 2.2 and 2.0 nm, respectively. The pore diameters derived from the adsorption isotherm are lower than the corresponding values obtained from the desorption isotherm by about 1 nm (Table 1). The surface area and total pore volume decrease significantly after co-condensation with increasing amount of APTS. The same behaviour was observed for ethylene-bridged silica modified by co-condensation of BTME with 3-glycidoxypropyltrimethoxysilane [21].

Co-incorporated APTS-modified ethylene-bridged silica. Shown in Figure 3 (A and B) are isotherms of the materials prepared by impregnating 0.3 g samples of an APTS-modified ethylene-bridged silica [(BAE(1:1), BET surface area = 389 m² g⁻¹, and pore volume = 0.27 cm³

g^{-1}] with 0.1 and 0.2 g of cobalt nitrate, yielding materials with 6.7 % [6.7CoBAE(1:1)] and 13.5 % [13.5CoBAE(1:1)] cobalt, respectively. The shape of the isotherm is not affected by post reaction cobalt incorporation. The effect of incorporating cobalt nitrate onto amine-functionalized materials on the surface area is clearly observed from the isotherms. The surface area and total pore volume decreased significantly after cobalt incorporation (Table 1). The decrease in surface area and pore volume as the amount of Co loading increases suggests that Co particles were deposited in the pores of the organosilica materials [56].

The surface areas and pore volumes of the materials prepared by the impregnation method are lower than the corresponding values of the materials prepared by the *in situ* procedure (see Table 1). For example, the cobalt incorporated APTS-modified ethylene-bridged silica material synthesized in the presence of 0.1 g cobalt nitrate [6.7CoBAE(1:1) - *in situ*] has a higher surface area ($308 \text{ m}^2/\text{g}$) compared to the material impregnated with an equivalent amount of cobalt nitrate ($250 \text{ m}^2/\text{g}$ for 6.7CoBAE(1:1) - *imp*). This arises since in the impregnation method all the Co nitrate fill the pores while in the *in situ* method some of the Co is incorporated in the framework to form Co-O-Si bonds and hence the Co does not block the pores as effectively.

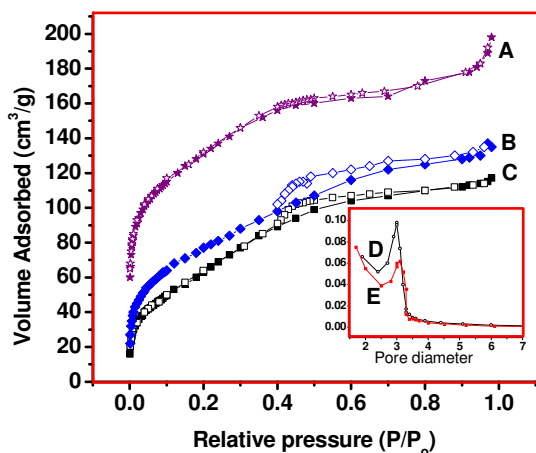


Figure 2. N_2 adsorption-desorption isotherms and BJH pore size distributions derived from desorption isotherms for APTS-modified ethylene-bridged silica and Co-incorporated APTS-modified ethylene-bridged silica materials. A, B and C are isotherms of APTS-modified ethylene-bridged silica with BTME:APTS mole ratios of 1:0.5, 1:0.7, and 1:1, respectively. D and E are BJH desorption PSDs for BAE1:1 and BAE(1:0.5), respectively.

Thermogravimetric analysis

APTS-modified ethylene-bridged silica. TGA (under N_2) was used to monitor the decomposition characteristics of the APTS-modified ethylene-bridged silica materials before and after solvent extraction. Analysis was conducted from room temperature to $1000 \text{ }^\circ\text{C}$. Thermograms and derivative thermograms of samples prepared from a mixture of APTS and BTME are shown in Figure 4. The results for as-synthesized and solvent extracted APTS-modified ethylene-bridged silica materials prepared from a mixture with BTME:APTS = 1:1 are summarised in Table 2. The profiles indicate that the organosilica materials all have similar thermal stability, with distinct mass losses, associated with the organic groups in the materials. Whereas the extracted

ethylene-bridged silica loses no weight in the range 262 – 370 °C [21], the solvent extracted APTS-modified ethylene-bridged silica materials lose mass in this region (Figure 4). The mass loss in this region decreases with decreasing amount of APTS used during synthesis and is consequently attributed to loss of the aminopropyl functional group. The onset of aminopropyl group decomposition overlaps with the decomposition of surfactant molecules in as-synthesized materials. The mass losses obtained in the temperature range 100 – 400 °C for materials with BTME:APTS mole ratios of 1:1 and 1:0.5 [BAE(1:1) and BAE(1:0.5)] are 17 and 24 %, respectively. All extracted APTS/BTME samples lose between 10 and 12 % of their masses due to framework ethylene group decomposition at temperatures between 400 and 800 °C. Another observation is that APTS/BTME samples lose more weight (due to methanol and ethanol desorption) below 100 °C compared to BTME samples. This is expected as the material formed from co-condensation of APTS and BTME is more hydrophilic than that prepared from BTME alone [26].

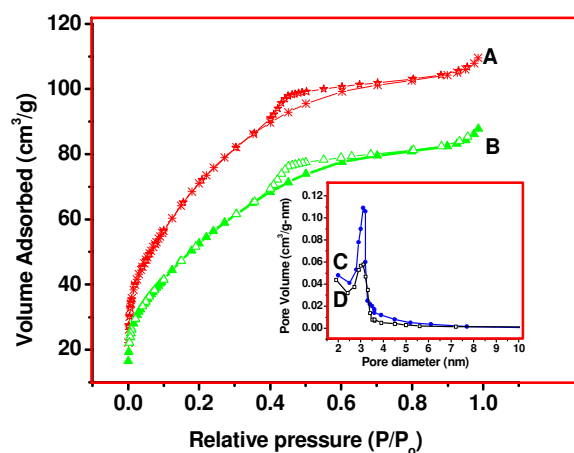


Figure 3. N₂ adsorption-desorption isotherms and BJH pore size distributions derived from desorption isotherms for Co-incorporated APTS-modified ethylene-bridged silica materials. A and B are isotherms of APTS-modified ethylene-bridged silica with BTME:APTS mole ratio of 1:1 impregnated with 6.7 % and 13.5 % cobalt, respectively. C and D are BJH desorption PSDs for 6.7CoBAE(1:1)-*imp* and 13.5CoBAE(1:1)-*imp*, respectively.

Table 2. TGA results of as-synthesized and solvent-extracted APTS-modified ethylene-bridged silica materials prepared from a mixture with BTME:APTS = 1:1.

Temperature range (°C)	% Mass loss of as synthesized material	% Mass loss of solvent extracted material	Source of mass loss
25 – 175	5 %	10 %	Desorption of water, ethanol and methanol
175 – 250	50 %	2 %	Surfactant decomposition
250 – 370	17 %	13 %	Decomposition of surfactant and aminopropyl functional group
370 – 600	5.5 %	12 %	Decomposition of ethylene groups from the ethylene-bridged silica network

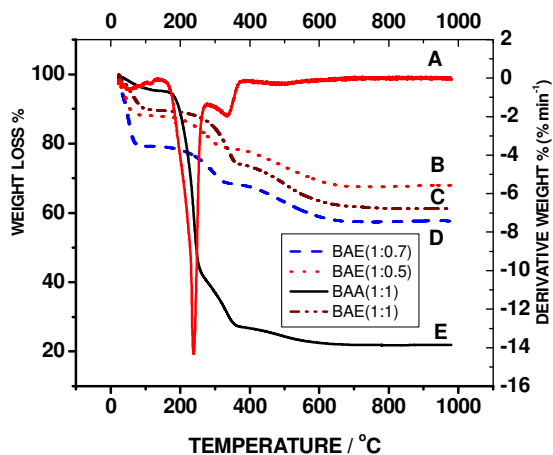


Figure 4. TGA curves and derivative thermograms for APTS-modified ethylene-bridged silica materials. A = derivative TGA curve of BAE(1:1); B, C, D and E are TGA curves of BAE(1:0.5), BAE(1:1), BAE(1:0.7) and BAA(1:1), respectively.

Co-incorporated APTS-modified ethylene-bridged silica. TGA curves of cobalt incorporated ethylene-bridged silica materials prepared by impregnation of 0.3 g ethylene-bridged silica samples with 0.1 and 0.2 g cobalt nitrate are shown in Figure 5. The mass loss at temperatures between 100 and 300 °C observed in materials obtained by impregnation is due to loss of products associated with the decomposition of the nitrate ions and water. Sample 6.7CoBAE(1:1) loses half (16 %) the mass lost by 13.5CoBAE(1:1) (30%) in agreement with the ratio of cobalt nitrate used for the impregnation. The other mass losses observed are similar to those associated with the hybrid support.

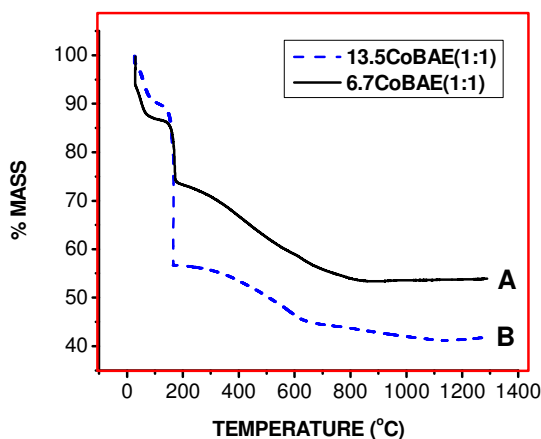


Figure 5. TGA curves for solvent extracted APTS-modified ethylene-bridged silica materials impregnated with cobalt nitrate. A = 6.7CoBAE(1:1) and B = 13.5CoBAE(1:1).

Raman spectroscopy

APTS-modified ethylene-bridged silica. Raman spectroscopy was used to identify functional groups associated with the new materials. Raman spectra of solvent extracted APTS-modified ethylene-bridged silica [BAE (1:0.5)] as well as solvent extracted ethylene-bridged silica (BE) are shown in Figure 6. After solvent extraction the peaks associated with CTAB had disappeared while those due to the C-H vibrations of the BTME and APTS ethylene groups (2885 cm^{-1}) are still to be seen (Figure 6) [57, 58]. The intensity of the Raman peaks indicative of the amine functional group, observed between 3250 and 3500 cm^{-1} , increases with an increasing amount of APTS in the reaction mixture. The absence of peaks between 600 and 700 cm^{-1} (which are observed in the spectra of silicon precursors) indicates considerable hydrolysis and condensation of the methoxy and ethoxy groups of the silicon precursors. Whereas single peaks are observed in the range $1200 - 1300$ (due to symmetric CH vibrations of Si-CH₂- groups) and $1400 - 1600\text{ cm}^{-1}$ (due to asymmetric CH vibrations of Si-CH₂- groups) in the spectrum of ethylene-bridged silica, doublets appear in the spectra of APTS-modified ethylene-bridged silica materials, indicating that the methylene groups in the framework and those due to the aminopropyl group are not equivalent (Figure 6). Bands due to Si-O vibrations are observed at 798 , 956 , 1078 and 1147 cm^{-1} .

Co-incorporated APTS-modified ethylene-bridged silica. Incorporation of Co into ethylene-bridged silica and APTS-modified ethylene-bridged silica yielded a material that has peaks at 686 cm^{-1} and at 480 cm^{-1} , indicative of Co₃O₄ [59]. However, no evidence for the presence of Si-O-Co-O-Si species was evident.

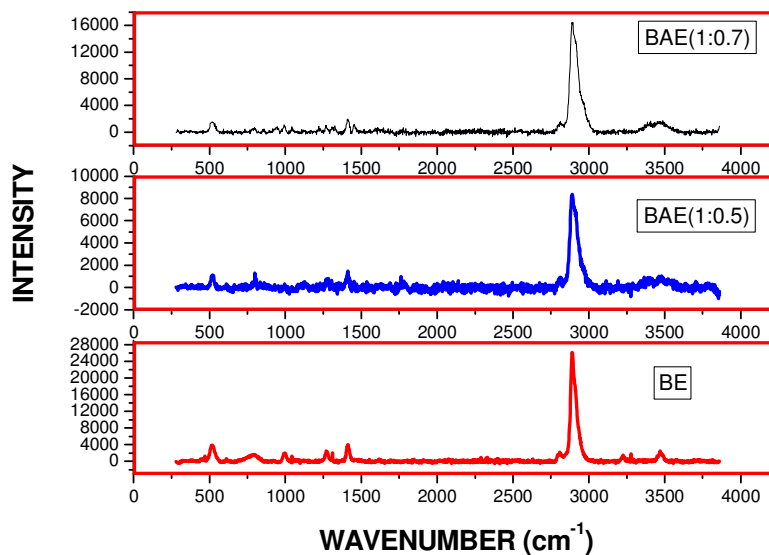


Figure 6. Raman spectra for solvent extracted ethylene-bridged silica (BE) and APTS-modified ethylene-bridged silica [BAE(1:0.5) and BAE(1:0.7)] materials.

UV-Vis diffuse reflectance spectroscopy

Co-incorporated APTS-modified ethylene-bridged silica. UV-Vis diffuse reflectance spectra of aminopropyl-modified ethylene-bridged silica materials impregnated with cobalt nitrate (0.1 and 0.2 g cobalt precursor per 0.3 g organosilica) as well as that of unsupported cobalt nitrate hexahydrate are presented in Figure 7. The absorption band at 428 nm is due to the formation of Co_3O_4 , where a migration of Co to octahedral sites has occurred [59]. The UV-vis diffuse reflectance spectroscopy thus confirms the presence of Co_3O_4 .

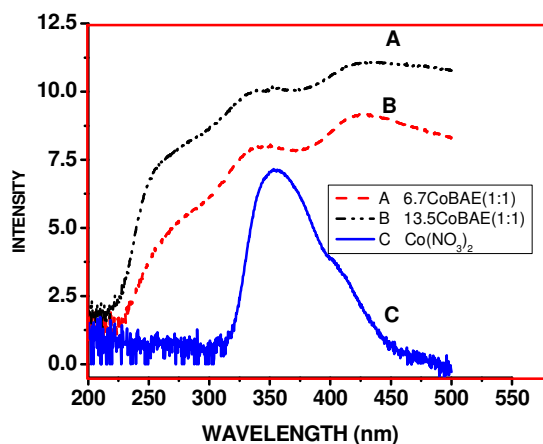


Figure 7. UV-VIS diffuse reflectance spectra of unsupported cobalt nitrate and supported cobalt nitrate.

Scanning electron microscopy (SEM)

APTS-modified ethylene-bridged silica. Typical scanning electron microscopy (SEM) images of ethylene-bridged silica, APTS-modified ethylene-bridged silica and cobalt incorporated APTS-modified ethylene-bridged silica materials are shown in Figure 8. The SEM image of an ethylene-bridged silica sample displays predominantly spherical particles with diameters in the range 11.1 to 21.8 μm . Smaller particles, with diameters ranging between 1.67 and 3.89 μm , dominate after modifying ethylene-bridged silica with APTS.

Co-incorporated APTS-modified ethylene-bridged silica. Cobalt impregnated materials, 6.7CoBAE(1:1) and 13.5CoBAE(1:1), show spherical particles with diameters in the 1.67 – 5.56 μm and 0.6 – 4.7 μm range, respectively. Particles with “shell-like” morphology are also observed for cobalt impregnated materials.

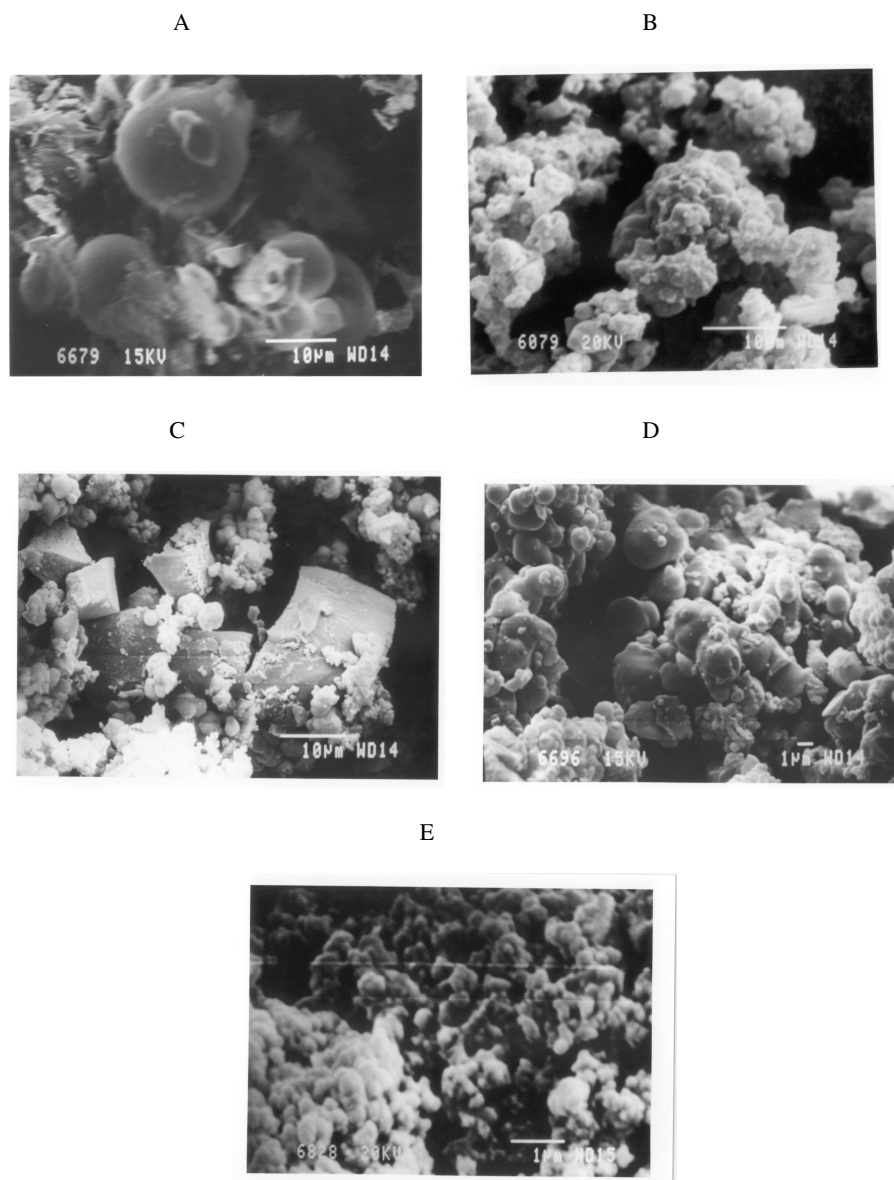


Figure 8. SEM micrographs of ethylene-bridged silica, APTS-modified ethylene-bridged silica and cobalt incorporated APTS-modified ethylene-bridged silica materials. A = ethylene-bridged silica (BE), B = *In situ* Co incorporated ethylene-bridged silica [6.7CoBAE(1:1) - *in situ*], C = APTS-modified ethylene-bridged silica [BAE(1:0.7)], D = cobalt impregnated APTS-modified silica [6.7CoBAE(1:1) - *imp*], and E = Cobalt impregnated APTS-modified ethylene-bridged silica [13.4CoBAE(1:1) - *imp*].

CONCLUSIONS

Bifunctional periodic mesoporous organosilica materials consisting of ethylene groups (in the framework) and aminopropyl groups in the channels were synthesized. Cobalt incorporated APTS-modified ethylene-bridged silica materials were synthesized *in situ* by adding cobalt nitrate to the reaction mixture. Cobalt was also supported on APTS-modified materials by using the incipient wetness impregnation method. Cobalt incorporation led to a collapse in the periodicity of the materials, as shown by the disappearance of the XRD peak observed at $2\theta = 2^\circ$. Cobalt ion incorporation was confirmed by Raman spectroscopy and UV-vis diffuse reflectance spectroscopy. The amount of APTS and cobalt incorporation determined the pore size, surface area and pore volume of the new material in a predictable manner.

ACKNOWLEDGEMENTS

We wish to thank the NRF, THRIP, Sastech, the University, the Mellon Foundation and DAAD for financial assistance.

REFERENCES

1. Sayari, A.; Hamoudi, S. *Chem. Mater.* **2001**, 13, 3151.
2. Melde, B.J.; Holland, B.T.; Blanford, C.F.; Stein, A. *Chem. Mater.* **1999**, 11, 3302.
3. Sayari, A.; Hamoudi, S.; Yang, Y.; Moudrakovski, I.; Ripmeester, J.R. *Chem. Mater.* **2000**, 12, 3857.
4. Guan, S.; Inagaki, S.; Ohsuna, T.; Terasaki, O. *J. Am. Chem. Soc.* **2000**, 122, 5660.
5. Inagaki, S.; Guan, S.; Fukushima, Y.; Ohsuna, T.; Terasaki, O. *J. Am. Chem. Soc.* **1999**, 121, 9611.
6. Guan, S.; Inagaki, S.; Ohsuna, T.; Terasaki, O. *Micropor. Mesopor. Mater.* **2001**, 44 – 45, 165.
7. Kruk, M.; Jaroniec, M.; Guan, S.; Inagaki, S. *J. Phys. Chem. B* **2001**, 105, 681.
8. Fan, H.; Reed, S.; Baer, I.; Schunk, R.; López, G.P.; Brinker, C.J. *Micropor. Mesopor. Mater.* **2001**, 44 – 45, 625.
9. Lu, Y.; Fan, H.; Doke, N.; Loy, D.A.; Assink, R.A.; LaVan, D.A.; Brinker, C.J. *J. Am. Chem. Soc.* **2000**, 122, 5258.
10. Fan, H.; Lu, Y.; Stump, A.; Reed, S.T.; Baer, T.; Schunk, R.; Perez-Luna, V.; López, G.P.; Brinker, C.J. *Nature* **2000**, 405, 56.
11. Park, S.S.; Lee, C.H.; Cheon, J.H.; Choe, S.J.; Park, D.H. *Bull. Korean Chem. Soc.* **2001**, 22, 948.
12. Lee, C.H.; Park, S.S.; Choe, S.J.; Park, D.H. *Micropor. Mesopor. Mater.* **2002**, 46, 257.
13. Muth, O.; Schellbach, C.; Froba, M. *Chem. Commun.* **2001**, 2032.
14. Cho, E-B.; Kwon, K-W.; Char, K. *Chem. Mater.* **2001**, 13, 3837.
15. Zhu, H.; Jones, D.J.; Zajac, J.; Rozière, J.; Dutartre, R. *Chem. Commun.* **2001**, 2568.
16. Burleigh, M.C.; Markowitz, M.A.; Wong, E.M.; Lin, J-S.; Gaber, B.P. *Chem. Mater.* **2001**, 13, 4411.
17. Matos, J.R.; Kruk, M.; Mercuri, L.P.; Jaroniec, M.; Asefa, T.; Coombs, N.; Ozin, G.A.; Kamiyama, T.; Terasaki, O. *Chem. Mater.* **2002**, 14, 1903.
18. Ren, T.; Zhang, X.; Suo, J. *Micropor. Mesopor. Mater.* **2002**, 54, 139.
19. Sayari, A.; Yang, Y. *Chem. Commun.* **2002**, 21, 2582.
20. Hamoudi, S.; Kaliaguine, S. *Chem. Comm.* **2002**, 18, 2118.

21. Tshavhungwe, A.M.; Layh, M.; Coville, N.J. *J. Sol-Gel Sci. Technol.* **2004**, *29*, 167.
22. Wahab, M.A.; Kim, I.; Ha, C-S. *Micropor. Mesopor. Mater.* **2004**, *69*, 19.
23. Asefa, T.; Kruk, M.; MacLachlan, M.J.; Coombs, N.; Grondy, H.; Jaroniec, M.; Ozin, G.A. *J. Am. Chem. Soc.* **2001**, *123*, 8520.
24. Burleigh, M.C.; Markowitz, M.A.; Spector, M.S.; Gaber, B.P. *Langmuir* **2001**, *17*, 7923.
25. Burleigh, M.C.; Markowitz, M.A.; Spector, M.S.; Gaber, B.P. *Chem. Mater.* **2001**, *13*, 4760.
26. Burleigh, M.C.; Markowitz, M.A.; Spector, M.S.; Gaber, B.P. *J. Phys. Chem. B* **2001**, *105*, 9935.
27. Burleigh, M.C.; Dai, S.; Hagaman, E.W. *Chem. Mater.* **2001**, *13*, 2537.
28. Hamoudi, S.; Kaliaguine, S. *Micropor. Mesopor. Mater.* **2003**, *59*, 195.
29. Hamoudi, S.; Kaliaguine, S. *Stud. Surf. Sci. Catal.* **2003**, *146*, 473.
30. Zhu, H.; Jones, D.; Zajac, J.; Dutartre, R.; Rhomari, M.; Roziere, J. *Chem. Mater.* **2002**, *14*, 4886.
31. Yuan, X.; Lee, H.I.; Kim, J.W.; Yie, J.E.; Kim, J.M. *Stud. Surf. Sci. Catal.* **2003**, *146*, 477.
32. Yuan, X.; Lee, H.I.; Kim, J.W.; Yie, J.E.; Kim, J.M. *Chem. Lett.* **2003**, *32*, 650.
33. Asefa, T.; Kruk, M.; Coombs, N.; Grondy, H.; MacLachlan, M.J.; Jaroniec, M.; Ozin, G.A. *J. Am. Chem. Soc.* **2003**, *125*, 11662.
34. Wight, A.P.; Davis, M.E. *Chem. Rev.* **2002**, *102*, 3589.
35. Macquarrie, D.J.; Clark, J.H.; Lambert, A.; Mdoe, J.E.G.; Priest, A. *React. Funct. Polym.* **1997**, *35*, 153.
36. Angeletti, E.; Canepa, C.; Martinetti, C.; Venturello, P. *Tetrahedron Lett.* **1988**, *29*, 2261.
37. Lasperas, M.; Llorett, T.; Chaves, L.; Rodriguez, I.; Cauvel, A.; Brunel, D. *Stud. Surf. Sci. Catal.* **1997**, *10875*.
38. Bigi, F.; Carloni, S.; Maggi, R.; Mazzacani, A.; Sartori, G. *Stud. Surf. Sci. Catal.* **2000**, *130*, 3501.
39. Demicheli, D.; Maggi, R.; Mazzacani, A.; Righi, P.; Sartori, G.; Bigi, F. *Tetrahedron Lett.* **2001**, *42*, 2401.
40. Ohtsuka, Y.; Arai, T.; Takasaki, S.; Tsubouchi, N. *Energy Fuels* **2003**, *17*, 804.
41. Panpranot, J.; Goodwin Jr., J.G.; Sayari, A. *J. Catal.* **2002**, *211*, 530.
42. Bian, G.; Machizuki, T.; Fujishita, N.; Namoto, H.; Yamada, M. *Energy Fuels* **2003**, *17*, 8799.
43. Cardiano, P.; Sergi, S.; Lazzari, M.; Piraino, P. *Polymer* **2002**, *43*, 6635.
44. Young, R.S. *Cobalt: Its Chemistry, Metallurgy and Uses*, American Chemical Society: Reinhold, New York; **1960**.
45. Withers Jr., H.P.; Eliezer, K.F.; Mitchell, J.W. *Ind. Eng. Chem. Res.* **1990**, *29*, 1807.
46. Iglesia, E. *Appl. Catal. A* **1997**, *161*, 59.
47. Brady, R.C.; Pettit, R.J. *J. Am. Chem. Soc.* **1981**, *103*, 1287.
48. Goodwin Jr., J.G. *Prep. ACS Div. Pet. Chem.* **1991**, *36*, 156.
49. Li, J.; Coville, N.J. *Appl. Catal. A* **2001**, *208*, 177.
50. Beck, J.S.; Vartuli, J.C.; Roth, W.J.; Leonowicz, M.E.; Kresge, C.T.; Schmitt, K.D.; Chu, C. T-W.; Olson, D.H.; Sheppard, E.W.; McCullen, S.; Higgins, J.B.; Schlenker, J.L. *J. Am. Chem. Soc.* **1992**, *114*, 10834.
51. Kresge, C.T.; Leonowicz, M.E.; Roth, W.J.; Vartuli, J.C.; Beck, J.S. *Nature* **1992**, *359*, 710.
52. Stein, A.; Melde, B.J.; Schrodin, R.C. *Adv. Mater.* **2000**, *12*, 1403.
53. Lim, M.H.; Blanford, C.F.; Stein, A. *Chem. Mater.* **1999**, *11*, 3285.
54. Tshavhungwe, A.M.; Coville, N.J. *J. Sol-Gel Sci. Technol.* **2004**, *31*, 161.
55. Gregg, S.J.; Sing, K.S.W. *Adsorption, Surface Area and Porosity*, Academic Press: London; **1982**.
56. Panpranot, J.; Goodwin Jr., J.; Sayari, A. *Catalysis Today* **2002**, *77*, 269.

57. Li, J.; Coville, N.J.; *Appl. Catal. A* **1999**, 181, 201.
58. Bois, A.; Bonhommé, L.; Ribes, A.; Pais, B.; Raffin, G.; Tessier, F. *Colloids and Surfaces A: Physicochem. Eng. Aspects* **2003**, 22, 1221.
59. Colthup, N.B.; Daly, L.H.; Wiberley, S.E. *Introduction to Infrared and Raman Spectroscopy*, 3rd ed., Academic Press: London, **1997**.
60. Mekhemer, G.A.H.; Abd-Allah, H.M.M.; Mansour, S.A.A. *Colloids and Surfaces A: Physicochem. Eng. Aspects* **1999**, 160, 251.